Article accepted for publication in IEEE/CAA Journal of Automatica Sinica,

# A Sensorless State Estimation for A Safety-Oriented Cyber-Physical System in Urban Driving: Deep Learning Approach

Mohammad Al-Sharman, David Murdoch, Dongpu Cao, Chen Lv, Yahya Zweiri, Derek Rayside and William Melek

*Abstract* — **In today's modern electric Vehicles, enhancing the Safety-Critical Cyber-Physical (CPS) system's performance is necessary for the safe maneuverability of the vehicle. As a typical CPS system, the braking system is crucial for the vehicle design and safe control. However, precise state estimation of the brake pressure is desired to perform safe driving with a high degree of autonomy. In this paper, a sensorless state estimation technique of the vehicle's brake pressure is developed using a deep-learning approach. A Deep Neural Network (DNN) is structured and trained using special deep-learning training techniques, such as, dropout and rectified units. These techniques are utilized to obtain more accurate model for brake pressure state estimation applications. The proposed model is trained using real experimental training data which were collected via conducting real vehicle testing. The vehicle was attached to a chassis dynamometer while the brake pressure data were collected under random driving cycles. Based on these experimental data, the DNN is trained and the performance of the proposed state estimation approach is validated accordingly. The results demonstrate high-accuracy brake pressure state estimation with RMSE of 0.048 MPa.**

***Index Terms— Cyber-Physical System (CPS), Brake Pressure State Estimation, Deep Learning, Dropout Regularization Approach.***

## I. Introduction

WITH the rise of autonomous vehicles, Cyber Physical Systems (CPSs) have become a major research focus, with teams from academia, industry and government organizations studying them [1]-[4]. In Electric Vehicles (EV), the various subsystems of the EV, like communications, electric powertrain and energy management, sensors, the driver, and the environment all come together to form a tightly coupled, dynamically interacting system [5]-[11]. The resulting system has strong uncertainties, nonlinearities, and difficult to model interactions between its parts, making estimation and control of CPSs in EVs a difficult task.

For CPSs in EVs, we are concerned primarily with safety critical systems, such as the braking system [12, 13, 14]. Braking systems have benefitted from numerous technological advances in the last several decades, such as new control schemes, higher safety standards, and other electronic improvements [15, 16, 17]. With increased autonomy and control authority, however, it becomes increasingly important that the braking system be accurate and safe against faults. Braking control generally uses measurements of the hydraulic pressure in brakes to decide actions to be taken, measured by pressure sensors [18]. If a hardware or software fault occurs in these sensors, however, brake control can be compromised, leading to potentially dangerous safety issues. This can be circumvented by using high precision brake pressure state estimation, with the potential to evolve the system into a sensorless system with sufficiently accurate estimation [19, 20].

This type of estimation has been a hot research topic in the past, generally through the use of control theory-based approaches. A recursive least-squares approach was used in [21] to estimate brake pressure by using characteristics of the pressure response of antilock braking systems. An Extended Kalman Filter based approach, combining tire dynamics and hydraulic models, was used in [22]. Other approaches have included the design of inverse models for brake pressure [23], modeling the decrease, increase, and hold of brake pressure using experimental data [24], including measuring the amount of fluid passing through the valve to determine brake pressure [25]. All of these, however, are controls based approaches, with none being suitable for a fully sensor-less design. [26] uses a neural net to perform estimation of brake pressure, using data obtained from an EV. However, this paper used conventional back propagation, which suffers from problems with overfitting, vanishing gradient, as well as higher computational complexity in training. Nevertheless, these problems have been resolved by implementing the recent advances of Deep Learning techniques to augment the training process of the DNN [27].

Deep learning can be described as a learning approach that employs DNNs which comprise of two or more hidden layers [28]. Deep learning was introduced to resolve the problems associated with the poor training techniques used with DNNs [29]. Among these problems are the overfitting and vanishing gradient problem. The vanishing gradient problem has been resolved using rectified unit functions as activation functions [30]. The overfitting problem has also been tackled by implementing modern regularization techniques, such as dropout [31]. Dropout randomly drops units and their connections during the weight update cycle to reduce overfitting. Similar results were found by [32], which used rectified linear units (ReLU) and dropout techniques to improve the accuracy of their neural net. These advantages are exploited to improve the training accuracy of the DNN and enhance the brake pressure state estimation.

Deep learning techniques are commonly used in the field of

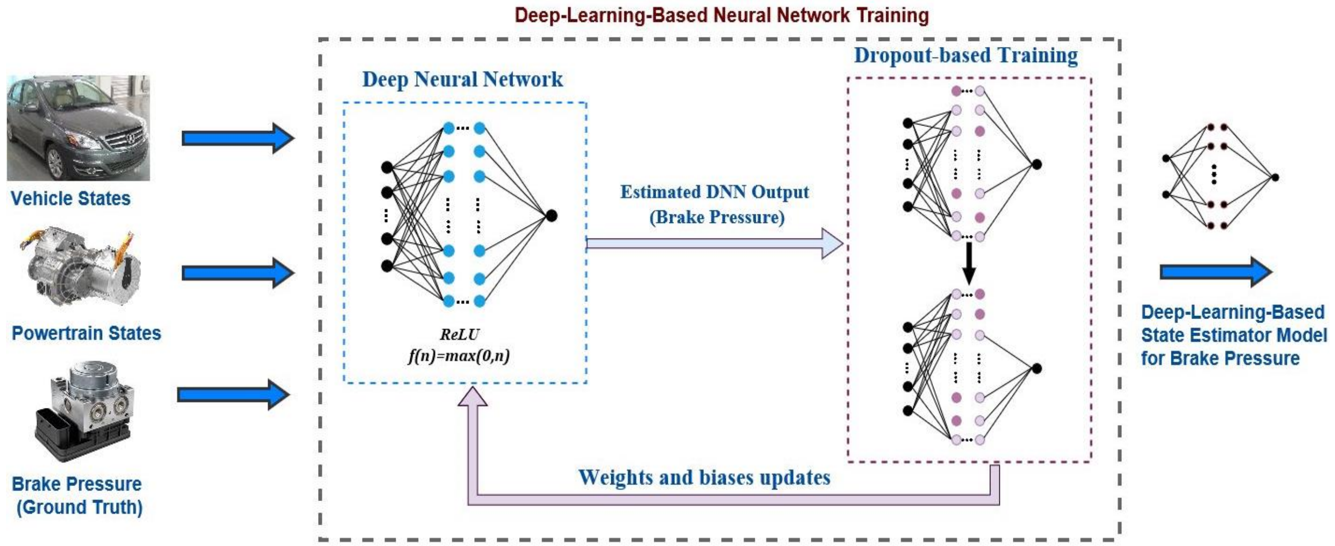

Figure 1:Deep-Learning-Based Training Technique

intelligent vehicles, most commonly in perception algorithms [33, 34, 35]. In past years, networks like AlexNet [36] and GoogLeNet [37] have achieved good results using deep learning for image classification, with image segmentation networks like YOLO9000 [38] and SSD [39] coming to the fore. Deep learning is also being used prominently in various forms in industrial applications. Fault detection and classification is an active research topic, with deep learning being used both to identify faults and to classify them, as well as for learning features to be used in fault classification [40, 41]. LiftingNet uses a multilayer neural network to extract deep features from noisy data for use in fault classification in motor bearings [42]. Other approaches have also been used, such as one that used unsupervised learning vibration images to perform intelligent feature extraction for fault diagnosis in rotor systems [43]. Semi-supervised learning is a more common approach, with one approach using semi-supervised learning based on hierarchical extreme learning machines for soft sensor modelling [44].

In this paper, a sensorless deep-learning-based approach is proposed for precise state estimation of the brake pressure of the electric vehicles (see Fig. 1). The term “sensorless” refers to that there is no sensor required to capture the changes in the braking pressure cycle while driving. Due to immense noise associated with the onboard vehicle’s sensors, developing sensorless data-driven estimation algorithm is highly needed to design robust control schemes [26, 45]. To the best of the authors’ knowledge and after exploring the existent literature, utilizing recent DL techniques for state estimation of brake pressure has not been addressed. The main novel contributions of the proposed state estimation algorithm can be concluded as follow: 1) A sensorless novel deep-learning-based algorithm is developed for brake pressure state estimation of an electric vehicle; 2) This state estimation technique uses current DL techniques and functions, such as dropout and ReLU to provide overfitting-free models of the state estimator; 3) The implementation of the proposed network is based on experimental data acquired using a real experimental vehicle testing environment; 4) Compared with conventional training methods, the proposed approach demonstrate more accurate brake pressure state estimation with RMSE errors of 0.048 MPa; 5) The proposed deep learning structure is expandable, hence, it can estimate other EV states in urban and high-way environments.

The rest of the paper is formed as follows. Section II reviews the structure of the DNN, dropout and Adam optimization technique. Section III illustrates the experimental setup and data collection system. Section IV presents the proposed DL brake pressure estimation technique. In Section V, the preliminary results of the proposed brake pressure state estimation approach. In Section IV, the proposed and the future works are presented.

## II. Deep Neural Network Design

Neural networks have demonstrated good performance for state estimation of the brake pressure [26]. However, obtaining highly expressive state estimator’s model is linked, in practice, to the accuracy of the utilized training method. Despite the effectiveness of conventional training techniques, modern deep-learning-based structures have shown superiority in terms of minimizing the associated overfitting and achieving fast convergence. In this section, a Deep Neural Network (DNN) is proposed using dropout regularization to improve the quality of the brake pressure estimation. As described in Fig. 1, the DNN uses the vehicle states and powertrain states as inputs and the ground truth of the brake pressure values are the outputs while conducting the training experiment of the neural network. In this section, the standard structure of the DNN is illustrated. Dropout and the ADAM optimization technique are also presented.

### A. *Deep Neural Networks*

A deep neural network was chosen in this study to perform brake pressure state estimation. Figure 2 illustrates the basic architecture design of the Multilayer Neural Network which is composed of a single input layer, one or more hidden layers and a single output layer.

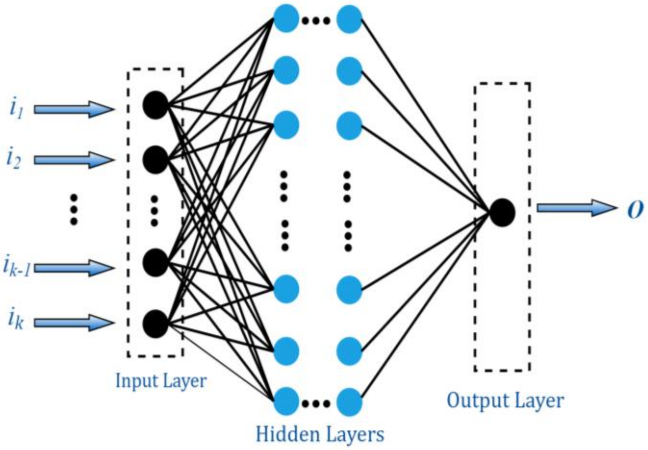

Figure 2: Structure of Multilayer Neural Network

The elements of the input vector $I = [i_1, i_2, \dots, i_k\ ]$ are weighted by the weight matrix $W$ and then summed with the neuron bias $b$ to yield the net input $n$.

$$n = \sum_{j=1}^{k} w_j i_j + b \tag{1}$$

Then the neuron output $a$ is generated using an activation function $f$.

$$a = \ f(n) \tag{2}$$

### B. *Conventional Training*

The backpropagation algorithm is commonly used for updating the weights of the NN. The operation of a neural network can be described using the equation:

$$a^{m+1}\ = \boldsymbol{f}^{m+1}(\boldsymbol{W}^{m+1} a^m + \boldsymbol{b}^{m+1}\ ) \tag{3}$$

where $a^m$ and $a^{m+1}$ represent the outputs of the *mth* and *m+1th* layers of the FFNN, and $\boldsymbol{b}^{m+1}$ is the bias weights for the *m+1th* layer. While training, the aim is to train the network with associations between the specific input-output mappings $\{(p_1, t_{1)}, \dots (p_Q, t_Q)\}$, where $p$ is the input vector and $t$ is the associated output. The Backpropagation algorithm adopts the Mean Squared Error (MSE) as the performance index for optimization, which can be approximated as

$$F(x)\ = e^T(k) e(k) \tag{4}$$

The steepest descent algorithm, using F as above, is then

$$w_{i,j}^m(k+1) = w_{i,j}^m(k) - \alpha \frac{\partial F}{\partial w_{i,j}^m} \tag{5}$$

$$b_i^m(k+1) = b_i^m(k) - \alpha \frac{\partial F}{\partial b_i^m} \tag{6}$$

where α is the learning rate. Defining the sensitivity of $F$ to changes in the *ith* element of the net input at layer *m* as

$$s_i^m = \frac{\partial F}{\partial n_i^m}\,, \tag{7}$$

the derivatives in (6) and (7) can then be simplified to

$$\frac{\partial F}{\partial w_{i,j}^m} = \ s_i^m a_j^{m-1} \tag{8}$$

$$\frac{\partial F}{\partial b_i^m} = \ s_i^m, \tag{9}$$

which then allows for the approximate steepest descent to be described in matrix form as a Jacobian with form

$$\frac{\partial \mathbf{n}^{m+1}}{\partial \mathbf{n}^m} = \begin{bmatrix} \frac{\partial n_1^{m+1}}{\partial n_1^m} & \cdots & \frac{\partial n_1^{m+1}}{\partial n_{s^m}^m} \\ \vdots & \ddots & \vdots \\ \frac{\partial n_{s^{m+1}}^{m+1}}{\partial n_1^m} & \cdots & \frac{\partial n_{s^{m+1}}^{m+1}}{\partial n_{s^m}^m} \end{bmatrix}, \tag{10}$$

where each element can be expressed as

$$\frac{\partial n^{m+1}}{\partial n^m} = \mathbf{W}^{m+1} \dot{\mathbf{F}}^{\mathrm{m}}(\boldsymbol{n}^m), \tag{11}$$

and

$$\dot{\mathbf{F}}^{\mathrm{m}}(\mathbf{n}^m) = \begin{bmatrix} \dot{f}^{\mathrm{m}}(n_1^m) & 0 & \cdots & 0 \\ 0 & \dot{f}^{\mathrm{m}}(n_2^m) & & 0 \\ \vdots & \vdots & & \vdots \\ 0 & 0 & \cdots & \dot{f}^{\mathrm{m}}(n_{s^m}^m) \end{bmatrix}. \tag{12}$$

The recurrence relation for $s^m$ can then be expressed using the chain rule

$$s^m = \frac{\partial F}{\partial \mathbf{n}^m} = \left(\frac{\partial \mathbf{n}^{m+1}}{\partial \mathbf{n}^m}\right)^T \frac{\partial F}{\partial \mathbf{n}^{m+1}}$$

$$= \ \dot{\mathbf{F}}^{\mathrm{m}}(\mathbf{n}^m)(\mathbf{W}^{m+1})^{\,T} s^{m+1}. \tag{13}$$

This relation can then be initialized at the final layer as

$$s_i^M = \frac{\partial \boldsymbol{F}}{\partial n_i^M} = \frac{\partial((\mathbf{t}-\mathbf{a})^T(\mathbf{t}-\mathbf{a}))}{\partial n_i^M}$$

$$= \frac{\partial \sum_{j=1}^{S^M}(t_j\ - a_j)^2}{\partial n_i^M}$$

$$= \ -2(t_i\ - a_i)\frac{\partial a_i}{\partial n_i^M}$$

$$= -2(t_i\ - a_i)\dot{f}^{\mathrm{m}}(n_i^m). \tag{14}$$

The final recurrence relation can thus be summarized as

$$s^M = -2\dot{\mathbf{F}}^M(\mathbf{n}^M)(\boldsymbol{t} - \mathbf{a}). \tag{15}$$

The training procedure of the neural network is deemed sensitive, and utilizing the conventional backpropagation (BP) as a stand-alone training approach may result in inaccurate performance of the obtained model [46]. BP experiences some problems pertaining to overfitting and computational complexity, which was recently tackled using some innovative DL training techniques, namely the use of dropout.

### *C. Dropout-Based training*

This section illustrates the basic Dropout neural network model. Dropout is a DL technique that was introduced as a simple way to resolve the problem of overfitting [27]. As shown in Fig.3, Dropout considers randomly selected units for training rather than all units [47].

In each layer $m$, $p^m$ denotes a vector of independent Bernoulli random variables which represents the probability of the dropped-out nodes. This vector is multiplied element-wise with the output of the associated layer, $\mathrm{a}^m$, to form the thinned outputs, $\hat{\mathrm{a}}^m$, as

$$p_j^m \sim \mathrm{Bernoulli}(p) \tag{16}$$

$$\hat{\mathrm{a}}^m = p^m * \mathrm{a}^m \tag{17}$$

The feed-forward operation, with dropout, is formulated as

$$\mathrm{a}^{m+1} = \mathbf{f}^{m+1}(\boldsymbol{W}^{m+1}\hat{\mathrm{a}}^m + \boldsymbol{b}^{m+1}). \tag{18}$$

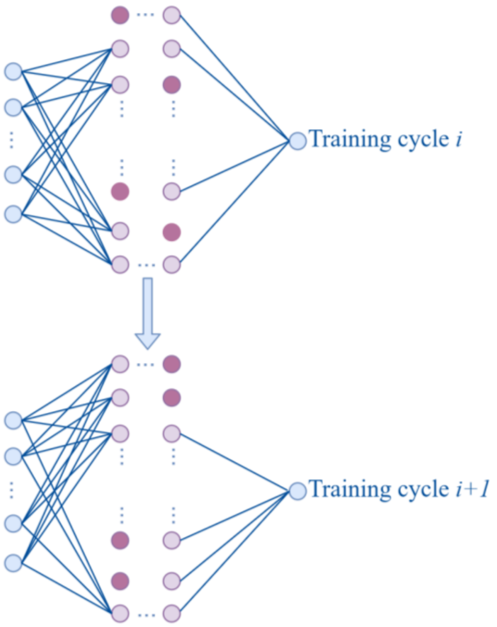

Figure 3: Dropout training technique

Dropout has shown its usefulness for Bayesian approximation and estimation purposes [48]. Incorporating adaptive gradient-based optimization techniques, such as, Adaptive Moment Estimation Technique (ADAM) with dropout has shown an excellent regression performance with a minimum training cost [49]. Hence, in this study, ADAM is adopted for gradient-based training optimization due to its fast convergence in regression problems compared to the conventional Stochastic Gradient Descent (SGD) [49].

Based on the estimation of the first and the second moment of the gradients, ADAM calculates the adaptive learning rates for specific parameters. The optimization algorithm has been considered suitable in applications where data contains a large number of parameters. ADAM optimization is also well-suited to state estimation problems where the measurements are associated with immense noise sequences and sparse gradients [49]. Fig. 4 represents the flowchart of the ADAM optimization scheme. $\alpha$ and $t$ define the step size and time step; respectively. $\theta_0$, $m_0$ and $v_0$ represent the initial parameter vector, 1st and second moment vectors.

The main aim of the ADAM optimization technique is to minimize the expected value of the noisy objective $f(\theta)$ with regard to its parameters $\theta$. $f_1(\theta)$,…, $f_N(\theta)$ represent the outputs of the stochastic function of following timestamps 1, ….., N. The sources of stochasticity might be associated with evaluation of the randomly selected batches of data points and/or from the associated noise sequence of the objective function. The vector of the partial derivatives of the objective function $f_t$ can be described as the gradient with respect to $\theta$.

$$g_t = \nabla_\theta f_t(\theta) \tag{19}$$

The squared gradient $(v_t)$ and the mean and the moving averages of $(m_t)$ the mean represent the estimates of the variance and the mean of the gradient, respectively. The exponential decay of these averages are controlled by using hyper-parameters $\beta_1$ and $\beta_2$.

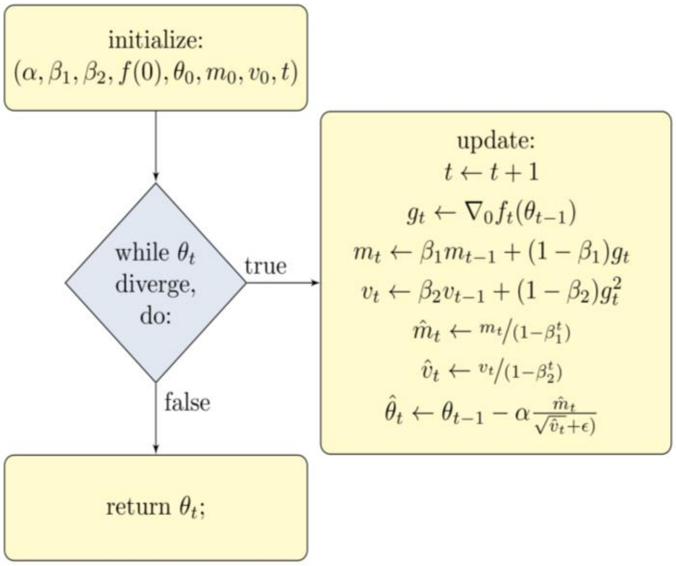
initialize:
$(\alpha, \beta_1, \beta_2, f(0), \theta_0, m_0, v_0, t)$
while $\theta_t$ diverge, do:
true
false
update:
$t \leftarrow t+1$
$g_t \leftarrow \nabla_0 f_t(\theta_{t-1})$
$m_t \leftarrow \beta_1 m_{t-1} + (1-\beta_1)g_t$
$v_t \leftarrow \beta_2 v_{t-1} + (1-\beta_2)g_t^2$
$\hat{m}_t \leftarrow m_t/(1-\beta_1^t)$
$\hat{v}_t \leftarrow v_t/(1-\beta_2^t)$
$\hat{\theta}_t \leftarrow \theta_{t-1} - \alpha\frac{\hat{m}_t}{\sqrt{\hat{v}_t + \epsilon)}}$
return $\theta_t$;

Figure 4: Adam Optimization scheme

## III. EXPERIMENTAL SETUP AND DATA COLLECTION

In this section, the experimental setup as well as the data collection procedure is presented. The proposed DNN is trained using real vehicle driving data. Several experiments were performed to collect training data using an electric passenger vehicle with a chassis dynamometer attached. The testing vehicle, data collection methods, selected feature methods, testing scenarios, and data pre-processing are described in the following sections.

### A. Testing vehicle and the electric powertrain

The data were collected via conducting real driving experiment using an electric car with chassis dynamometer, as exhibited in Fig.5. The chosen vehicle is driven by a permanent-magnet synchronous motor, which can operate either in driving or generating modes. The electric motor is powered via battery via a DC bus, which releases or absorbs the electric power during driving or braking cycles, respectively. Relevant specifications of the test vehicle and power train are shown in Table I.

Table 1: EV and Powertrain list of specs.

| | Specification | Value | Unit |
|---|---|---|---|
| Vehicle | Overall Mass | 1360 | kg |
| | Gear ratio | 7.881 | — |
| | Transmission efficiency | 96% | — |
| | Nominal radius of tire | 0.295 | m |
| | Coefficient of air Resistance | 0.32 | — |
| | Wheelbase | 2.50 | m |
| Battery | Voltage | 326 | V |
| | Capacity | 66 | Ah |
| Electric motor | Maximum torque | 144 | Nm |
| | Peak power | 45 | kW |

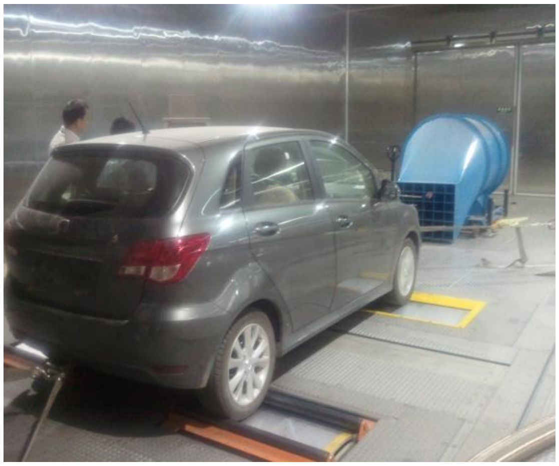

Figure 5: EV testing using a chassis dynamometer.

Several driving cycles standards can be used to set up the testing scenarios. The New European Drive Cycle (NEDC) which comprises of four repeated urban driving cycles was used for brake pressure estimation using NN [26]. However, arbitrary driving style imposes more challenges for NN to predict the brake pressure. In this paper, random driving cycles were adopted to better represent the urban driving environment with a range of speed up to 45 km/h. The proposed DL based brake pressure estimation is designed to capture the relevant trends of the urban driving behavior.

The electric powertrain comprises the fundamental components that generate electrical power. This comprehends a gearbox, an electric motor, a differential and a couple of two half shafts. At the center of the front axle, the electric motor is placed. In acceleration scenarios, accelerating the vehicle, the electric motor produces a propulsion torque that is transmitted to the axle to propel the vehicle through the drivetrain. While the electric motor switches to the regenerative brake mode to apply a braking toque in the vehicle deceleration scenarios [50, 51].

The hydraulic brake system installed in the testing vehicle includes wheel cylinders, a master brake cylinder, and inlet/outlet valves. As illustrated in Fig.6 which represents the hydraulic brake structure, a spring and a piston are used to model the wheel cylinder movements. Based on the hydraulic valve dynamics and fluid flow, the pressure of the wheel cylinder can be expressed by equation 20. Detailed models can be found in [1]:

$$\dot{p}_{FW} = \frac{k_{FW}}{\pi^2 r_{FW}^4} C_d A_v \sqrt{\frac{2 \cdot \Delta p}{\rho_{fluid}}} \qquad (20)$$

where $r_{FW}$ and $k_{FW}$ denote the radius of the piston and stiffness of the spring, respectively. $A_v$ is the cross section area of the valve opening and $C_d$ is the flow coefficient. $\Delta p$ and $\rho_{fluid}$ are the pressure difference across the valve and the density of the hydraulic fluid.

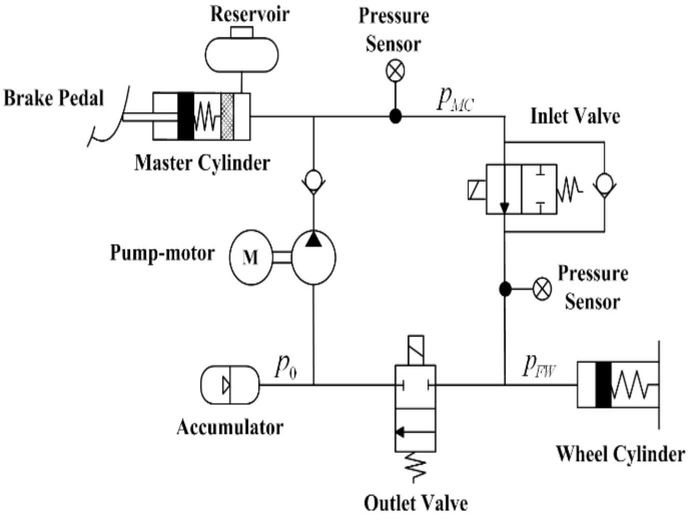

Figure 6: Structure of the hydraulic brake system.

### B. Data collection and preprocessing

The vehicle was run through several random driving cycles, giving a total of 10000 seconds of data. Vehicle states and powertrain data were collected using the CAN bus, at a frequency of 100 Hz. In order to enhance the training performance, the raw unbalanced features data were smoothed and subsequently scaled from 0 to 1 to reduce the effect of the dissimilar units of the used signals. Fig.7 shows an example of the collected raw data of the vehicle speed and corresponding brake pressure.

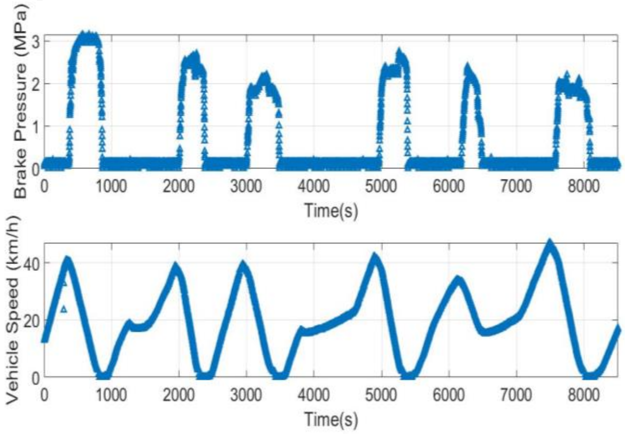

Figure 7: The vehicle speed and corresponding brake pressure.

### C. Process of feature selection

Selecting unique, and redundancy-free features contribute to a successful training of the state estimator model. The main states of the vehicle and powertrain were selected to train the model of brake pressure state estimator, while the measured brake pressure value is used as a ground truth. In addition to the vehicle and powertrain parameters, the motor speed and torque, the battery voltage and current, and the state of charge (SoC) of the battery are used as unique features. This is because when the EV is in the deceleration mode, the electric motor works as a generator, recapturing the kinetic energy. This causes the motor and battery current to change from positive to negative, which indicates that the battery is being recharged by regenerated energy from braking. The mean and standard deviations of some vehicle states are also added as features.

## IV. Deep learning based State estimator model

Obtaining precise state estimates in such highly dynamic systems is challenging due to sensor drifts and immense bias sequences [52, 53, 54]. In this section, the proposed deep-structured neural network is evaluated for the purpose of brake pressure state estimation. The scaled EV features along with the ground truth brake pressure are considered for the training process of the DNN. The proposed DNN uses the vehicle states and powertrain states and the ground truth brake pressure values as target outputs while training the DL state estimator model. Figure 8 illustrates some key features from the training data for one natural driving cycle.

Designing an accurate DL-Based state estimator model to estimate the brake pressure is not straightforward. Obtaining an accurate model is linked to the accuracy of the utilized training datasets, the structure of the network, training and optimization techniques. In this study, innovative deep learning techniques are exploited to enhance the training process of the DNN. Dropout regularization and Rectified Linear Units (ReLUs) are implemented to improve the prediction of the Brake pressure state estimator's model. As shown in Fig. 9, the proposed DNN consists of visible input and output layers and 3 hidden layers, along with the visible inputs and outputs layers.

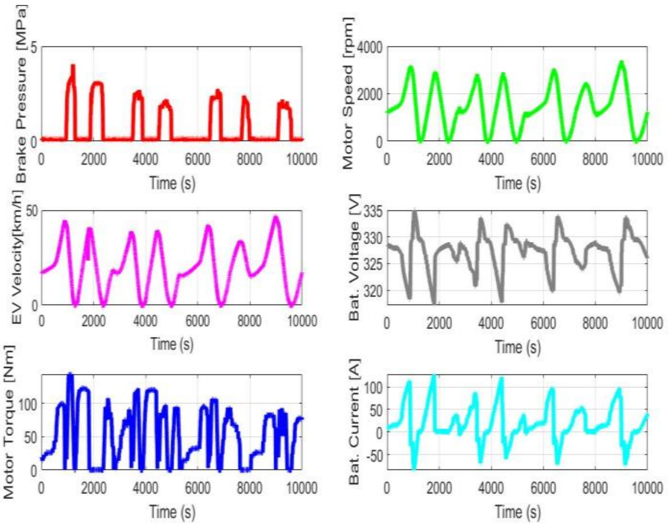

Figure 8: Sample of pre-scaled key features training data.

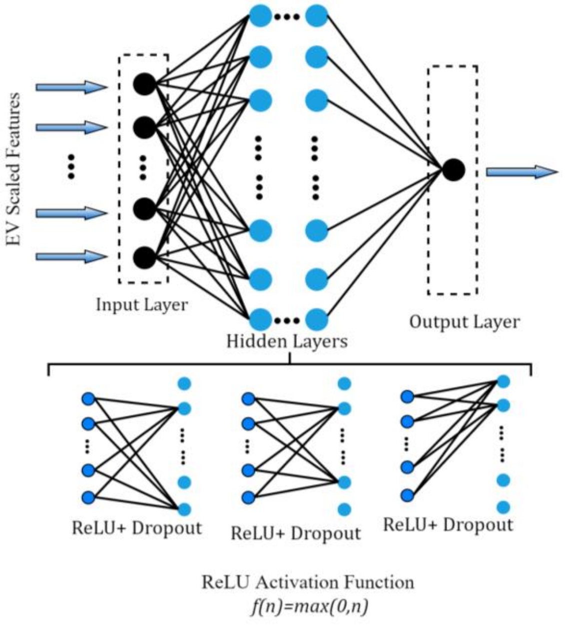

Figure 9: DNN Training Scheme

The ReLU activation function is used to generate the output signal of the hidden values, it can be expressed as follows:

$$f(n) = max(0, n) \tag{21}$$

The ReLU activation function is used to ensure accurate training for all hidden layers' nodes. Dropout regularization method is implemented to reduce the training cycle's computations by considering arbitrarily selected nodes for the training rather than the entire net. This means that the dropped-out units have temporally no contribution on the forward path and any weight updates are not applied to the neuron on the backward path. The implementation of dropout is not cumbersome; it is based on picking random units with a predefined probability (*p*) to be excluded from the training process. A low probability value has small impact and high values may cause under-learning by the network. However, with respect to the size of the DNN and number of units, a probability value of 10%-50% can provide good performance.

## V. Experimental Results and discussions

This section presents the training and testing results of the implemented DL-based approach for the brake pressure state estimation. Discussions of dropout probability tuning are also included.

### A. *State estimator model training*

The proposed brake pressure state estimation method is implemented in Python with Keras. Several DL models were developed and trained by importing the experimental data to the Keras environment. A DL structure of 3 hidden layers with 60, 40 and 20 neurons respectively, was chosen based on its smallest MSE of 0.087. All of the experiments shown were run on an AMD Radeon™ HD 6800 Series GPU. The ADAM optimization algorithm is used to update the weights and biases based on the Mean Squared Errors (MSE) loss function [55]:

$$MSE = \frac{1}{2\mathrm{N}}\sum_{k=1}^{n}(Y_k - \widehat{Y_k})^2 \tag{22}$$

where $Y_k$ and $\widehat{Y_k}$ are the target and evaluated network outputs; respectively, *N* represents the number of training data points.

Dropout technique can be implemented for the hidden layers as well as for the visible layers. In order to investigate the best implementation with appropriate probability *p*, several batch training tests are performed with probabilities ranging from 0.1 to 0.5. The tests are performed with dropout being applied to both the visible input layer alone, and to the visible input and the hidden layers. Figure 10 exhibits the average RMSE values over 200 epochs for both cases. As can be seen, the RMSE values increases as the dropout probability increases. It can be noticed that dropout is more feasible to be incorporated for hidden and visible input layers, based on the lower RMSE values. The dropout probability can be optimized through cross validation.

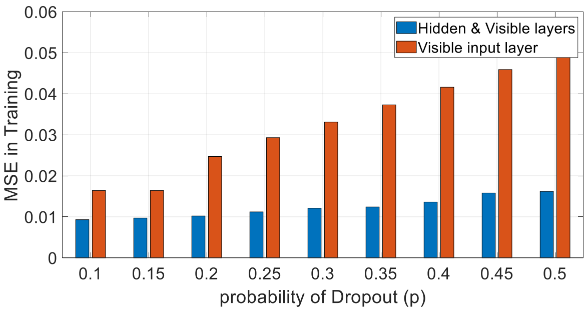

Figure 10: RMSE in validation with different dropout probabilities

The proposed model is trained using 8500 experimental data points over 200 epochs. Fig. 11 illustrates the accuracy of the training performance of the DNN. As shown, the losses represented by MSE values decrease as the DNN's weights and biases updated. This proves the accurate update of the weight and biases while training the DNN. Based on the small MSE values, it can be concluded that the training process has obtained an expressive neural network model based on the training set used.

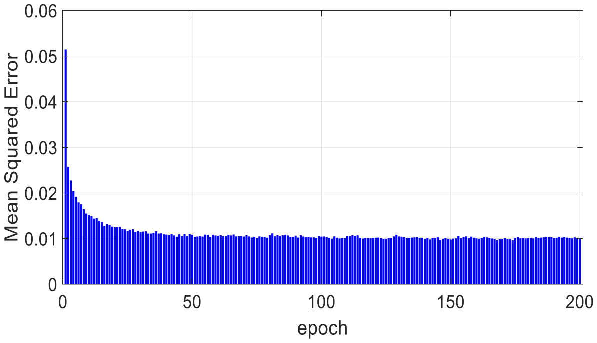

Figure 11: MSE in training over 200 epochs

### B. *State estimator model testing*

In this section, the proposed DL-Based state estimation algorithm is tested and evaluated. A testing environment is developed for the trained model. A 20 % of the collected data points was selected for testing the proposed state estimator model. The testing data includes the vehicle states and the power train states. The output of the proposed DL-based state estimator has been compared to the ground truth values of the brake pressure. Fig. 12 shows the scaled brake pressure state estimation. The x-axis represents the number of samples while the y-axis represents the scaled brake pressure. As can be observed, the results of the proposed DL-based state estimation approach show a significant coincidence with the ground truth values of the brake pressure.

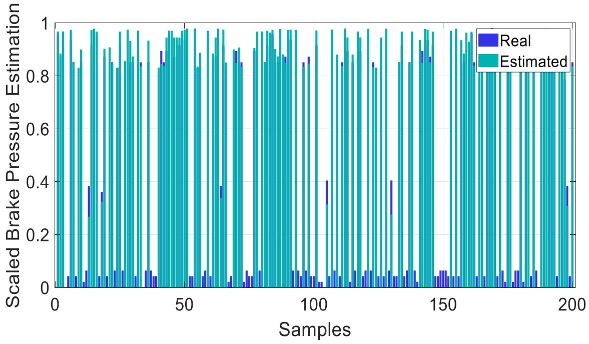

Figure 12: DL-Based Brake Pressure state estimation

Figure 13 shows the state estimation error magnitudes. To evaluate the accuracy of the proposed approach, regression performance errors are quantified using two main indices, namely, the RMSE and the coefficient of determination $R^2$. $R^2$ is a measure of the model's predication accuracy. It falls between 0 and 1, and the higher the value of the coefficient $R^2$, the better the model at predicting the observations. $R^2$ is described as

$$R^2 = 1 - \frac{\sum_{i=1}^{n}(\,y_i - \hat{y}_i)^2}{\sum_{i=1}^{n}(\,y_i - \bar{y}_i)^2} \tag{23}$$

where $\hat{y}$ represents the predicated values of the state $y$ and $\bar{y}$ represent the mean value of the state.

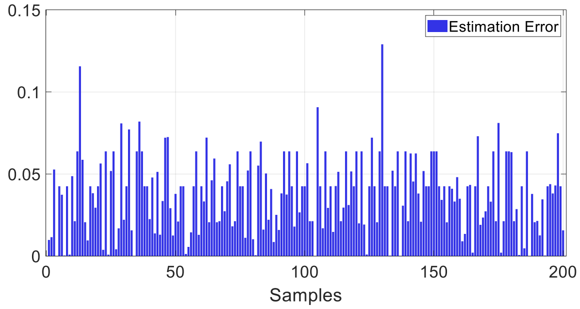

Figure 13: Error values of the proposed state estimation method

The proposed model has achieved a regression accuracy with $R^2$ of 0.994, indicating that the proposed model of the brake pressure state estimator can achieve high predication-accuracy of the brake pressure. Compared with the conventional training technique [26], the proposed has achieved more accurate state estimation with RMSE of 0.048 MPa. Based on the presented results, the proposed method demonstrates an accurate sensorless brake pressure state estimation.

## VI. Conclusion

This paper proposes a novel DL-based state estimation algorithm for a safety-critical cyber-physical system. Using dropout and other DL modern elements such as ReLU activation functions, a novel DL-based model is introduced for brake pressure state estimation purposes. Real experiments for data collection are conducted via testing the EV on a chassis dynamometer under random driving cycles. The obtained data of the powertrain systems and vehicle states, as well as the ground truth values of the brake pressure are used for the training process. The DL-based state estimator model is trained using dropout with different probabilities. The training results show a high fitting accuracy. The trained model is tested and the performance of brake pressure state estimation technique is evaluated. The state estimation results demonstrate the applicability and effectiveness of the proposed brake pressure state estimation approach.

As a future work of this research, the proposed state estimation can be further implemented and integrated with the onboard brake control system. The proposed DL-based model can also be flexibly expanded to estimate other states of the vehicle under several road conditions in urban and high-way scenarios. Furthermore, the estimated brake pressure information can be utilized in designing decision-making schemes for optimal braking in complex urban multiagent driving environment.

## VII. References

[1] C. Lv, Y. Liu, X. Hu, H. Guo, D. Cao and F.-Y. Wang , "Simultaneous Observation of Hybrid States for Cyber-Physical Systems: A Case Study of Electric Vehicle Powertrain," *IEEE Transactions on Cybernetics,* vol. 48, no. 8, pp. 2357 - 2367, 2018.

[2] J. Lee, B. Bagheri and H.-A. Kao, "A Cyber-Physical Systems architecture for Industry 4.0-based manufacturing systems," *Manufacturing Letters,* vol. 3, pp. 18-23, 2015.

[3] G. Xiong , F. Zhu , X. Liu , X. Dong , W. Huang, S. Chen and K. Zhao, "Cyber-physical-social system in intelligent transportation," *IEEE/CAA Journal of Automatica Sinica,* vol. 2, no. 3, pp. 320 - 333, 2015.

[4] L. Li, X. Peng, F.-Y. Wang, D. Cao and L. Li, "A situation-aware collision avoidance strategy for car-following," *IEEE/CAA Journal of Automatica Sinica,* vol. 5, no. 5, pp. 1012 - 1016, 2018.

[5] Y. Li , C. Lv, J. Zhang, Y. Zhang and W. Ma, "High-Precision Modulation of a Safety-Critical Cyber-Physical System: Control Synthesis and Experimental Validation," *IEEE/ASME Transactions on Mechatronics,* vol. 23, no. 6, pp. 2599 - 2608, 2018.

[6] H. Wang, Y. Huang and A. Khajepour , "Cyber-Physical Control for Energy Management of Off-Road Vehicles With Hybrid Energy Storage Systems," *IEEE/ASME Transactions on Mechatronics,* vol. 23, no. 6, pp. 2609 - 2618, 2018.

[7] F.-Y. Wang, N.-N. Zheng, D. Cao, C. M. Martinez, L. Li and T. Liu, "Parallel Driving in CPSS: A Unified Approach for Transport Automation and Vehicle Intelligence," *IEEE/CAA Journal of Automatica Sinica,* vol. 4, no. 4, pp. 577-587, 2017.

[8] T. Liu, X. Tang, H. Wang, H. Yu and X. Hu , "Adaptive Hierarchical Energy Management Design for a Plug-In Hybrid Electric Vehicle," *IEEE Transactions on Vehicular Technology,* vol. 68, no. 12, pp. 11513 - 11522, 2019.

[9] T. Liu, X. Hu, W. Hu and Y. Zou, "A Heuristic Planning Reinforcement Learning-Based Energy Management for Power-Split Plug-in Hybrid Electric Vehicles," *IEEE Transactions on Industrial Informatics,* vol. 15, no. 12, pp. 6436 - 6445, 2019.

[10] T. Liu, B. Wang and C. Yang, "Online Markov Chain-based energy management for a hybrid tracked vehicle with speedy Q-learning," *Energy,* vol. 160, pp. 544-555, 2018.

[11] T. Liu, H. Yu, H. Guo, Y. Qin and Y. Zou, "Online Energy Management for Multimode Plug-In Hybrid Electric Vehicles," *IEEE Transactions on Industrial Informatics,* vol. 15, no. 7, pp. 4352 - 4361, 2019.

[12] J. . J. Castillo, J. . A. Cabrera, A. J. Guerra and A. Simón , "A Novel Electrohydraulic Brake System With Tire–Road Friction Estimation and Continuous Brake Pressure Control," *IEEE Transactions on Industrial Electronics* , vol. 63, no. 3, pp. 1863 - 1875 , 2015.

[13] A. Dadashnialehi, A. Bab-Hadiashar, Z. Cao and A. Kapoor, "Intelligent Sensorless Antilock Braking System for Brushless In-Wheel Electric Vehicles," *IEEE Transactions on Industrial Electronics,* vol. 62, no. 3, pp. 1629 - 1638 , 2015.

[14] M. Ataei , A. Khajepour and S. Jeon, "Application of Adaptive Sliding Mode Control for Regenerative Braking Torque Control," *IEEE/ASME Transactions on Mechatronics,* vol. 23, no. 5, pp. 2031 - 2041, 2012.

[15] C. Qiu, G. Wang, M. Meng and Y. Shen, "A novel control strategy of regenerative braking system for electric vehicles under safety critical driving situations," *Energy,* vol. 149, pp. 329-340, 2018.

[16] L. Wang, Z. Zhan, X. Yang, Q. Wang , Y. Zhang, L. Zheng and G. Guo, "Development of BP Neural Network PID Controller and Its Application on Autonomous Emergency Braking System," in *IEEE Intelligent Vehicles Symposium (IV)* , Changshu, 2018 .

[17] J. Tan, C. Xu, L. Li, F.-Y. Wang, D. Cao and L. Li, "Guidance control for parallel parking tasks," *IEEE/CAA Journal of Automatica Sinica,* vol. 7, no. 1, pp. 301 - 306, 2020.

[18] Y. Li, C. Tang, S. Peeta and Y. Wang, "Integral-Sliding-Mode Braking Control for Connected Vehicle Platoon: Theory and Application," *IEEE Transactions on Industrial Electronics,* vol. Early Access, 2018.

[19] A. Dadashnialehi, A. Bab-Hadiashar, Z. Cao and R. Hoseinnezhad, "Reliable EMF-Sensor-Fusion-Based Antilock Braking System for BLDC Motor In-Wheel Electric Vehicles," *IEEE Sensors Letters,* vol. 1, no. 3, 2017.

[20] H. Guo, H. Guo, H. Chen, C. Lv, H. Wang and S. Yang, "Vehicle Dynamic State Estimation: State of the Art Schemes and Perspectives,"

*IEEE/CAA Journal of Automatica Sinica,* vol. 5, no. 2, pp. 418-431, 2017.

[21] N. Ding and X. Zhan, "Model-Based Recursive Least Square Algorithm for Estimation of Brake Pressure and Road Friction," in *Proceedings of the FISITA 2012 World Automotive Congress*, Berlin, 2012.

[22] G. Jiang, X. Miao, Y. Wang, D. Li, L. Liu and F. Muhammad, "Real-time estimation of the pressure in the wheel cylinder with a hydraulic control unit in the vehicle braking control system based on the extended kalman filter," *Proceedings of the Institution of Mechanical Engineering, Part D: Journal of automobile Engineering,* vol. 231, no. 10, pp. 1340-1352, 2017.

[23] L. Li, J. Song and Z. Han, "Hydraulic Model and Inverse Model for Electronic Stability Program Online Control System," *Chinese Journal of Mechanical Engineering,* vol. 44, no. 2, 2008.

[24] J. Zhang, C. Lv, J. Gou and D. Kong, "Cooperative control of regenerative braking and hydraulic braking of an electrified passenger car," *Proceedings of the Institution of Mechanical Engineers, Part D: Journal of Automobile Engineering,* vol. 226, no. 10, pp. 1289-1302, 2012.

[25] K. O'Dea, "Anti-lock braking performance and hydraulic brake pressure estimation," SAE World Congress, Michigan, 2005.

[26] C. Lv , Y. Xing, J. Zhang, X. Na, Y. Li, T. Liu, D. Cao and F.-Y. Wang, "Levenberg–Marquardt Backpropagation Training of Multilayer Neural Networks for State Estimation of a Safety-Critical Cyber-Physical System," *IEEE Transactions on Industrial Informatics,* vol. 14, no. 8, pp. 3436 - 3446, 2018.

[27] N. Srivastava, G. Hinton, A. Krizhevsky, I. Sutskever and R. Salakhutdinov, "Dropout: a simple way to prevent neural networks from overfitting," *Journal of Machine Learning Research,* vol. 15, pp. 1929-1958, 2014.

[28] Y. LeCun, Y. Bengio and G. Hinton, "Deep Learning," *Nature* , vol. 521, pp. 444-436, 2015.

[29] I. Gooodfellow, Y. Bengio and A. Courville , Deep Learning, Cambridge : MIT Press, 2016 .

[30] A. L. Maas, A. . Y. Hannun and A. Y. Ng, "Rectifier nonlinearities improve neural network acoustic models," in *International Conference on Machine Learning*, Georgia , 2013.

[31] P. Baldi and P. Sadowski, "The dropout learning algorithm," *Artificial Intelligence,* vol. 210, pp. 78-122, 2014.

[32] G. E. Dahl , T. N. Sainath and G. E. Hinton , "Improving deep neural networks for lvcsr using rectified linear units and dropout," in *International Conference on Acoustics, Speech and Signal Processing* , Vancouver, 2013.

[33] C. Yan, H. Xie , D. Yang, J. Yin, Y. Zhang and Q. Dai , "Supervised Hash Coding With Deep Neural Network for Environment Perception of Intelligent Vehicles," *IEEE Transactions on Intelligent Transportation Systems,* vol. 19, no. 1, pp. 284 - 295 , 2017.

[34] T. Liu, B. Tian , Y. Ai, Y. Zou and F.-Y. Wang, "Parallel reinforcement learning-based energy efficiency improvement for a cyber-physical system," *IEEE/CAA Journal of Automatica Sinica* , vol. (Early Access), pp. 1-10, 2019.

[35] L. Xu, "An overview and perspectives on bidirectional intelligence: Lmser duality, double IA harmony, and causal computation," *IEEE/CAA Journal of Automatica Sinica* , vol. 6, no. 4, pp. 865 - 893, 2019.

[36] A. Krizhevsky, I. Sutskever and G. . E. Hinton, "Imagenet classification with deep convolutional neural networks," in *Advances in Neural Information Processing Systems 25 (NIPS 2012)*, 2012.

[37] C. Szegedy, W. Liu, Y. Jia, P. Sermanet, S. Reed, D. Anguelov, D. Erhan, V. Vanhoucke and A. Rabinovich , "Going deeper with convolutions," in *IEEE Conference on computer vision and Pattern Recognition*, 2015.

[38] J. Redmon and A. Farhadi, "YOLO9000: Better, faster, stronger," in *IEEE Conference on Computer Vision and Pattern Recognition*, Honolulu , 2017.

[39] W. Liu, D. Anguelov, D. Erhan, C. Szegedy, S. Reed, C.-Y. Fu and A. Berg, "Ssd: Single shot multibox detector," in *European conference on computer vision*, Amsterdam , 2016.

[40] W. Lu, B. Liang, Y. Cheng, D. Meng, J. Yang and T. Zhang , "Deep Model Based Domain Adaptation for Fault Diagnosis," *IEEE Transactions on Industrial Electronics,* vol. 64, no. 3, pp. 2296 - 2305 , 2017.

[41] M. Xia , T. Li , L. Xu , L. Liu and C. W. de Silva, "Fault Diagnosis for Rotating Machinery Using Multiple Sensors and Convolutional Neural Networks," *IEEE/ASME Transactions on Mechatronics,* vol. 23, no. 1, pp. 101 - 110, 2018.

[42] J. Pan, Y. Zi, J. Chen , Z. Zhou and B. Wang , "LiftingNet: A Novel Deep Learning Network With Layerwise Feature Learning From Noisy Mechanical Data for Fault Classification," *IEEE Transactions on Industrial Electronics,* vol. 65, no. 6, pp. 4973 - 4982 , 2018.

[43] H. Oh, J. H. Jung, B. C. Jeon and B. D. Youn, "Scalable and Unsupervised Feature Engineering Using Vibration-Imaging and Deep Learning for Rotor System Diagnosis," *IEEE Transactions on Industrial Electronics,* vol. 65, no. 4, pp. 3539 - 3549 , 2018.

[44] L. Yao and Z. Ge, "Deep Learning of Semisupervised Process Data With Hierarchical Extreme Learning Machine and Soft Sensor Application," *IEEE Transactions on Industrial Electronics,* vol. 65, no. 2, pp. 1490 - 1498 , 2017.

[45] M. Al-Sharman, Y. Zweiri, M. Jaradat, R. Al-Husari, D. Gan and L. Seneviratne, "Deep-learning-based neural network training for state estimation enhancement: application to attitude estimation," *IEEE Transactions on Instrumentation and Measurement,* vol. 69, no. 1, pp. 24-34, 2019.

[46] J. Schmidhuber, "Deep learning in neural networks: An overview," *Neural Networks,* vol. 61, pp. 85-117, 2015.

[47] G. E. Dahl, T. N. Sainath and G. E. Hinton, "Improving deep neural networks for LVCSR using rectified linear units and dropout," in *IEEE International Conference on Acoustics, Speech and Signal Processing*, Vancouver, BC, 2013.

[48] Y. Gal and Z. Ghahramani, "Dropout as a Bayesian Approximation: Representing Model Uncertainty in Deep Learning," in *international conference on machine learning*, New York, 2016.

[49] D. P. Kingma and J. L. Ba, "ADAM: A METHOD FOR STOCHASTIC OPTIMIZATION," in *International Conference on Learning Representations*, San Diego , 2015.

[50] Y. Yuan, J. Zhang , Y. Li and C. Li, "A Novel Regenerative Electrohydraulic Brake System: Development and Hardware-in-Loop Tests," *IEEE Transactions on Vehicular Technology,* vol. 67, no. 12, pp. 11440 - 11452, 2018.

[51] C. Lv , Y. Xing , C. Lu, Y. Liu, H. Guo , H. Gao and D. Cao, "Hybrid-Learning-Based Classification and Quantitative Inference of Driver Braking Intensity of an Electrified Vehicle," *IEEE Transactions on Vehicular Technology,* vol. 67, no. 7, pp. 5718 - 5729, 2018.

[52] M. K. S. Al-Sharman, "Attitude Estimation for a Small-Scale Flybarless Helicopter," in *Multisensor Attitude Estimation: Fundamental Concepts and Applications*, CRC Press, 2016, pp. 513-528.

[53] K. Saadeddin, M. F. Abdel-Hafez and M. A. Jarrah, "Estimating Vehicle State by GPS/IMU Fusion with Vehicle Dynamics," *Journal of Intelligent and Robotic Systems: Theory and Applications,* vol. 74, no. 2, pp. 147-172, 2014.

[54] M. Al-Sharman, M. Al-Jarrah and M. Abdel-Hafez, "Auto takeoff and precision terminal-phase landing using an experimental optical flow model for GPS/INS enhancement," *ASCE-ASME Journal of Risk and Uncertainty in Engineering Systems, Part B: Mechanical Engineering,* vol. 5, no. 1, pp. 1-17, 2018.

[55] J. C. Principe, N. R. Euliano and W. C. Lefebvre, Neural and Adaptive Systems: Fundamentals through Simulations, New York: Wiley, 2000.

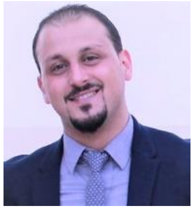

**Mohammad K. Al-Sharman** received the B.Sc. and M.Sc. degrees in mechatronics engineering from Tafila Technical University and American University of Sharjah in 2011 and 2015, respectively. He is currently working towards the Ph.D. degree in the Electrical and Computer engineering from the University of Waterloo, Canada. From 2015 to 2017, he was involved in several research activities where auto takeoff and precision landing using integrated sensors was developed for rotary wing UAVs. From 2017 to 2018, he was a Research Associate with the Robotics Institute, Khalifa University, UAE.

Mr. Al-Sharman has been a recipient of multiple academic scholarships and awards during his undergraduate and graduate studies. His current research areas include stochastic estimation, automated driving, machine learning and reinforcement learning for decision making applications. He is currently a reviewer for IEEE/ASME Transactions on Mechatronics and the IEEE Transactions on Instrumentation and Measurement, where he was recognized as one of Transactions "Outstanding Reviewers of 2019".

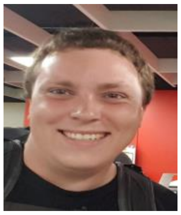

**David Murdoch** is currently working on his Masters in Applied Science in Mechanical and Mechatronics at the University of Waterloo. His research interests involve developing robust path planning techniques for autonomous aerial and ground vehicles. Before his Masters, he attended Waterloo and completed his B.Sc. degree in Computer Engineering.

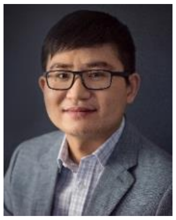

**Dongpu Cao** received the Ph.D. degree from Concordia University, Canada, in 2008. He is a Canada Research Chair in Driver Cognition and Automated Driving, and currently an Associate Professor and Director of Waterloo Cognitive Autonomous Driving (CogDrive) Lab at University of Waterloo, Canada. His current research focuses on driver cognition, automated driving and cognitive autonomous driving. He has contributed more than 200 publications, 2 books and 1 patent. He received the SAE Arch T. Colwell Merit Award in 2012, and three Best Paper Awards from the ASME and IEEE conferences. Dr. Cao serves as an Associate Editor for IEEE TRANSACTIONS ON VEHICULAR TECHNOLOGY, IEEE TRANSACTIONS ON INTELLIGENT TRANSPORTATION SYSTEMS, IEEE/ASME TRANSACTIONS ON MECHATRONICS, IEEE TRANSACTIONS ON INDUSTRIAL ELECTRONICS and ASME JOURNAL OF DYNAMIC SYSTEMS, MEASUREMENT AND CONTROL. He was a Guest Editor for VEHICLE SYSTEM DYNAMICS and IEEE TRANSACTIONS ON SMC: SYSTEMS. He serves on the SAE Vehicle Dynamics Standards Committee and acts as the Co-Chair of IEEE ITSS Technical Committee on Cooperative Driving.

**Chen Lv** (S'14-M'16) is an Assistant Professor of School of Mechanical and Aerospace Engineering, Nanyang Technological University, Singapore. He received the Ph.D. degree at Department of Automotive Engineering, Tsinghua University, China in 2016. He was a Research Fellow at Advanced Vehicle Engineering Center, Cranfield University, UK during 2016 and 2018, and a joint PhD researcher at EECS Dept., University of California, Berkeley, USA during 2014 and 2015. His research focuses on advanced vehicle control and intelligence, where he has contributed over 80 papers and obtained 12 granted China patents.

Dr. Lv serves as a Guest Editor for IEEE/ASME Transactions on Mechatronics, and IEEE Transactions on Industrial Informatics, and an Associate Editor for Plos One, Automotive Innovation, International Journal of Electric and Hybrid Vehicles, and International Journal of Vehicle Systems Modelling and Testing. He received the Highly Commended Paper Award of IMechE UK in 2012, the China SAE Outstanding Paper Award in 2015, the Tsinghua University Outstanding Doctoral Thesis Award in 2016, and the Best Workshop/Special Session Paper Award of IEEE Intelligent Vehicle Symposium in 2018.

**Yahya H. Zweiri** received the Ph.D. degree from King's College London, London, U.K., in 2003. He currently is an Associate Professor with Kingston University London, Kingston, U.K., and with Khalifa University, Abu Dhabi, UAE. He was involved in defense and security research projects for the last 20 years with the Defense Science and Technology Laboratory, Hampshire, U.K., King's College London, and King Abdullah II Design and Development Bureau, Amman, Jordan. He has authored over 100 refereed journal and conference papers; and filed five U.S. and GB patents in the unmanned systems field. His current research interests include the interaction dynamics between unmanned systems and unknown environments by means of deep learning, machine intelligence, constrained optimization, and advanced control.

**Derek Rayside** is an Associate Professor in the Electrical & Computer Engineering Department at the University of Waterloo, where he is also a faculty advisor (along with William Melek) to the Watonomous.ca autonomous vehicle team in the SAE AutoDrive Challenge. He is a member of SAE, IEEE, and ACM, and is a licensed P.Eng. in Ontario. He received the PhD from MIT's Department of Electrical Engineering and Computer Science, preceded by a MASc in Computer Engineering and a BASc in Systems Design Engineering, both from the University of Waterloo.

**William Melek** is the Director of Mechatronics Engineering and the RoboHub at the University of Waterloo. He is and an expert on robotics, artificial intelligence, sensing, and state estimation. He earned his doctorate in mechanical engineering from the University of Toronto in 2002, and then led the Artificial Intelligence Division of Alpha Laboratories Inc. He founded University of Waterloo Laboratory of Computational Intelligence and Automation in 2004 and was awarded the Young Engineer Medal of Professional Engineers Ontario in 2006. He is the past President of the North American Fuzzy Information Processing Society (NAFIPS), and a senior member of the Institute for Electrical and Electronics Engineers (IEEE). Dr. Melek developed Canada's first industry-ready modular reconfigurable robot (MMR); the state-of-the-art open architecture system is now used in the automotive sector. He has also led the way in designing practical, intelligent and adaptive control architectures for MMRs based on neural networks. Conceptual prototypes have been developed for the nuclear industry in the United States. He holds twelve Canadian and U.S. patents, and his contributions to the manufacturing industry have been featured in the National Post, Globe and Mail and CBC television.